THE ASTROPHYSICAL JOURNAL, 537:L43–L47, 2000 July 1

THE STARFISH TWINS: TWO YOUNG PLANETARY NEBULAE WITH EXTREME MULTIPOLAR MORPHOLOGY

RAGHVENDRA SAHAI
Jet Propulsion Laboratory, MS 183-900, California Institute of Technology,
4800 Oak Grove Drive, Pasadena, CA 91109; sahai@grandpa.jpl.nasa.gov
Received 2000 February 17; accepted 2000 April 6; published 2000 June 23

ABSTRACT

We present Hα images of two objects, He 2-47 and M1-37, obtained during a *Hubble Space Telescope* imaging survey of young planetary nebulae (PNs) selected on the basis of their low-excitation characteristics. The two objects show a highly aspherical morphology, characterized by multiple lobes distributed around the central star. Such a morphology has never been seen before in any astrophysical setting. Bright structures near the minor axes indicate the presence of dense equatorial tori (seen edge-on in M1-37 and as partial elliptical rings in He 2-47). In both nebulae, the central star is found to be offset from the geometrical center of symmetry of the waist region. The multiple lobes of He 2-47 and M1-37 have been produced fairly recently (a few hundred years ago), based on rough estimates of their expansion ages. The extreme multipolar morphology of these PNs supports the recent hypothesis of Sahai & Trauger that the primary agents for shaping PNs are high-speed collimated outflows that operate during the late asymptotic giant branch (AGB) and/or early post-AGB evolutionary phase; these outflows change their direction episodically, and/or multiple collimated outflows with different axes operate (quasi)simultaneously. Drastic modifications of existing theories or completely new ideas are needed in order to obtain a full understanding of the salient morphological features of He 2-47 and M1-37.

Subject headings: circumstellar matter — ISM: jets and outflows — planetary nebulae: individual (He 2-47, M1-37) — stars: AGB and post-AGB — stars: mass loss

1. INTRODUCTION

Most planetary nebulae (PNs) show a dazzling variety of aspherical morphologies (e.g., Balick 1987; Schwarz, Corradi, & Melnick 1992; Manchado, Stanghellini, & Guerrero 1996; Sahai & Trauger 1998, hereafter ST98), whereas the extended circumstellar envelopes (CSEs) of the progenitor asymptotic giant branch (AGB) stars appear to be largely round (e.g., Bowers, Johnston, & Spencer 1983; Sahai & Bieging 1993). Although there is no consensus on the physical mechanism or mechanisms responsible for shaping PNs, there is observational evidence that these are transitory in nature and that they occur during the earliest formation stages of PNs. We are therefore carrying out imaging studies of a number of young PNs and proto–planetary nebulae (PPNs; objects in transition from the AGB to the PN phase) using the *Hubble Space Telescope* (*HST*); the results obtained so far provide important constraints on the processes that shape PNs (ST98; Sahai, Bujarrabal, & Zijlstra 1999a; Sahai et al. 1999b, 1999c, 1999d; Sahai 1999, 2000).

In this Letter, we present *HST* images of two objects (He 2-47 and M1-37) obtained during our Hα imaging survey of young PNs. The very unusual multilobed morphologies that we find in He 2-47 and M1-37 have never been seen before in any astrophysical setting. These objects thus pose a very difficult problem for most current theories of PN formation and shaping (see Frank 2000 for a recent review), and they dramatically highlight the need for new theoretical developments in this field.

2. OBSERVATIONS AND RESULTS

He 2-47 and M1-37 were imaged using the Wide Field Planetary Camera 2 (WFPC2) on board the *HST* (guest observer proposal 6353); the target selection and observing strategy are described in ST98. All images were recorded through the F656N (Hα) filter using the 800 × 800 pixel^2 PC chip of WFPC2, which has a plate scale of 0.″0456 pixel^{-1}.

The Hα images of He 2-47 (also known as PK 285−02°1) and M1-37 (also known as PK 002−03°3 and He 2-339) are displayed in Figures 1 and 2. For each object, an image in which the sharp structures have been enhanced is also shown in false color. He 2-47 shows eight major lobes (labeled N1–N4 and S1–S4) with radial extents between 3.″7 and 4.″7 emanating from a dense waist (i.e., minor axis of the nebula) that is aligned along a position angle (P.A.) of 64° (*dotted line*, Fig. 1*b*). Lobes N1, N2 and S1, S2 are not as well differentiated from each other as the other lobes. Two small lobes (W1 and W2) are partially seen just beyond the waist's western edge, and a small part of one lobe (E1) is seen beyond the waist's eastern edge. The waist region contains two bright *partial* ringlike structures (*dashed curves*, Fig. 1*b*). The southeastern ring is significantly brighter than the northwestern one, indicating that the latter is the more distant one, with its brightness being attenuated by a larger column of nebular dust. The visible central star located in their interior is offset from the minor axis, toward the NW ring, by 0.″1 (along P.A. = −26°). The rings are well fitted by ellipses with major and minor axes equal to 1.″2 and 0.″77, respectively; if they are intrinsically circular, then the ring planes are tilted to our line of sight by 40°. M1-37, like He 2-47, also has a multipolar morphology (Fig. 2); at least seven lobes (labeled N1–N3 and S1–S4) with radial extents between 1.″8 and 2.″2 emanate from a dense waist. The waist, oriented at P.A. = 44° (Fig. 2*b*), is probably a torus seen roughly edge-on. The visible central star is offset from the waist center toward its northeast end by 0.″1. The bright multilobed nebulae are surrounded by faint, roughly round halos; the halo is more prominent in M1-37, which also shows a bright arc at the halo's northern periphery, 2.″6 from the center. The J2000 coordinates of the central stars, measured from

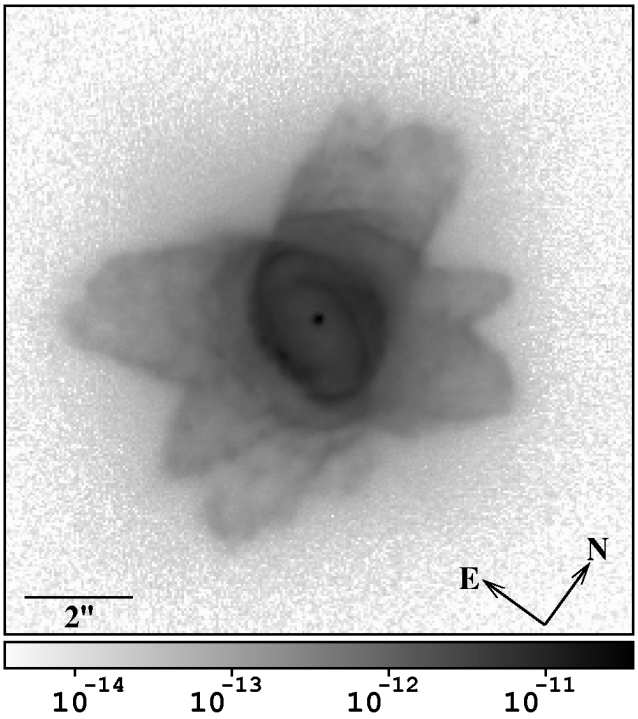

FIG. 1*a*

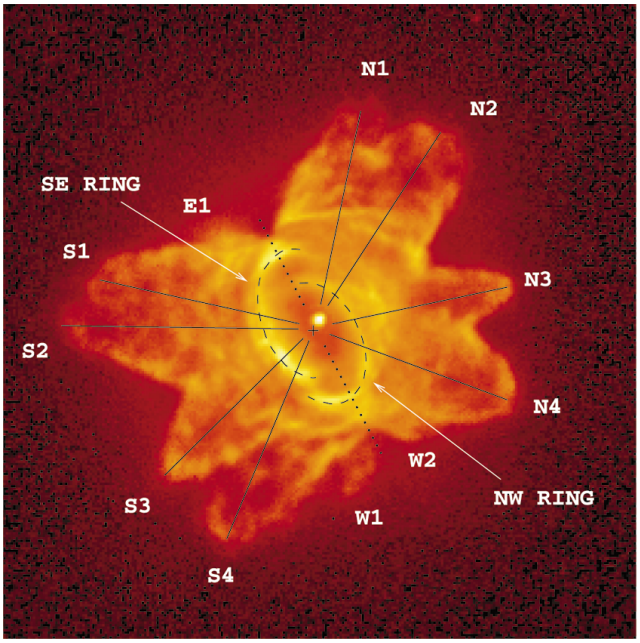

FIG. 1*b*

FIG. 1.—(*a*) Hα image of He 2-47, a low-excitation PN, taken with the WFPC2 on the *HST*. The reverse gray-scale image shows the Hα intensity on a logarithmic scale. The maximum and minimum surface brightnesses defining the black and white ends of the gray scale are 3.6×10^{-11} and 3.6×10^{-15} ergs s^{-1} cm^{-2} arcsec^{-2}, respectively. (*b*) False-color image, which shows the data in the left panel processed to enhance sharp structures. The processed image, $Im_P = Im_O/(Im_O + 0.04Im_S)$, where Im_O is the original image and Im_S is obtained by smoothing Im_O. The very faint regions are coded in red, whereas the brighter regions are coded in orange and yellow. Various structural features described in the text (§ 2) are labeled, and the geometric center of symmetry of the waist region is marked with a cross. The dotted line shows the minor axis, and the radial vectors indicate the position angles of selected lobes.

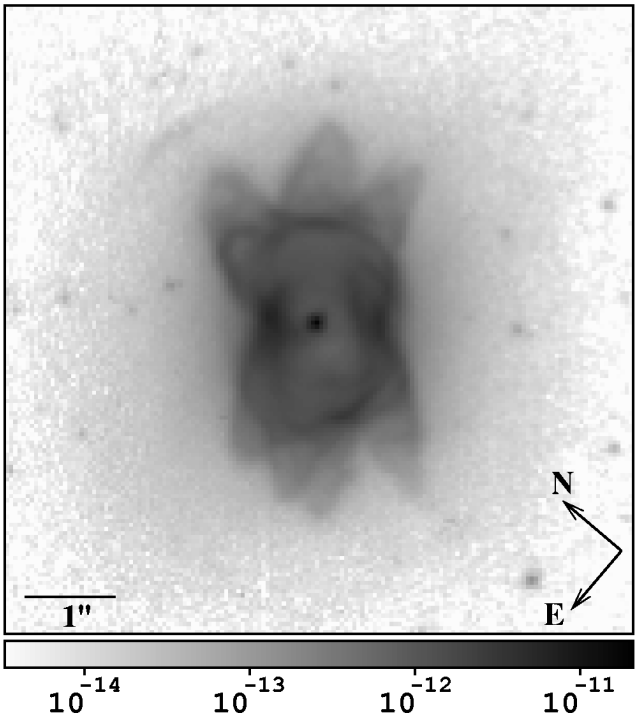

FIG. 2*a*

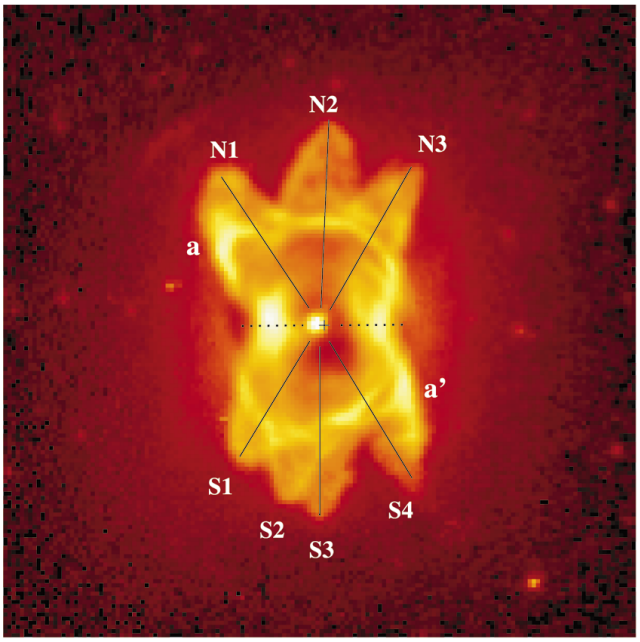

FIG. 2*b*

FIG. 2.—Same as in Fig. 1, but for the low-excitation PN M1-37. The maximum and minimum surface brightnesses are 2.1×10^{-11} and 3.3×10^{-15} ergs s^{-1} cm^{-2} arcsec^{-2}, respectively.

our images, are $\alpha = 10^h23^m09^s.21$, $\delta = -60°32'41''.53$ for He 2-47 and $\alpha = 18^h05^m25^s.725$, $\delta = -28°22'04''.21$ for M1-37.

The two rings in He 2-47 appear to be point-symmetric about a common geometric center, which is offset from the central star by 0″.21 (*cross*, Fig. 1*b*). Similarly, the bright curved edges of lobes N1 and S4 in M1-37 (labeled *a* and *a′* in Fig. 2*b*) are also located point-symmetrically around the waist's geometric center (*cross*, Fig. 2*b*). Drawing vectors from a point midway between the geometric center and the central star to the tips of the major lobes in each object, we find that in He 2-47, lobes N1–N4 are related to lobes S1–S4 *roughly via reflection symmetry* about the nebular waist. The same relationship holds between the two sets of lobes N1, N2, N3 and S1, S3, S4 in M1-37; however, a point-symmetric configuration pairing up N1 with S4, N2 with S3, and N3 with S1 is equally plausible.

A comparison of the fluxes of both PNs at different wavelengths indicates that they are intrinsically similar in size and brightness but are located at different distances. We find that the stellar blue and visual (continuum) fluxes, the Hα flux, and the *IRAS* 25 μm flux of He 2-47 are higher than that of M1-37 by factors of 6.3, 6.3, 5.5, and 7.5, respectively, implying that He 2-47 is a factor of 2.55 ± 0.2 times closer than M1-37. Consistent with this conclusion, we find that the angular size of the waist region of He 2-47 is a factor of 2.5 times larger than that of M1-37. In view of their shapes and their similarity to each other, we hereby dub He 2-47 and M1-37 as the *Starfish Twins*.

If we adopt a distance D of 2 kpc for He 2-47 (Maciel 1984), then the distance to M1-37 is 5 kpc, consistent with the value listed by Acker et al. (1992). Given these distances, we can make rough estimates of the densities (which scale as $D^{-0.5}$) in different nebular regions from the Hα surface brightness (assuming case B recombination and an electron temperature of 10^4 K). The scattered stellar continuum contribution to the image intensities is negligible based on typical central-star effective temperatures for low-excitation PNs [(3–4) $\times$ 10^4 K; Zhang & Kwok (1991) give $T_{\rm eff} = 3.78 \times 10^4$ K for M1-37] and the luminosities for our objects (see § 3). In each object, the lobes show evidence for limb brightening, indicating that the density near their peripheries is larger than in their interiors (Figs. 1 and 2). Assuming that the lobes are axially symmetric structures, we find the radial Hα emission of each lobe by taking a radial intensity cut through the lobe symmetry axis and subtracting from it a similar *halo intensity* cut from a neighboring region outside the lobe. Thus, e.g., in lobe S3 (S4) of He 2-47, we find the density at the lobe edge to be about 3.9 (4.6) $\times$ 10^3 cm^{-3}, dropping by a factor of 2.4 (1.8) in its interior; for lobe N2 of M1-37, the lobe-edge density is 2.8×10^3 cm^{-3}, dropping by a factor of 1.6 in its interior. In this analysis, we have taken care to avoid regions where lobes overlap. Since we are using *average* densities to estimate the density contrasts between the lobe edges and interiors, the actual contrast factors must be higher. For example, if we model lobe N2 of M1-37 as a partially evacuated cavity with a dense wall of thickness $\lesssim$0″.1, then the wall-to-interior density ratio is $\gtrsim$5. Lobe masses can be roughly estimated by assuming them to be prolate semiellipsoids with bases coinciding with the nebular waists and by multiplying the resulting volumes with their average interior densities (estimated above); we thus obtain masses of 3.5×10^{-3} and 6.5×10^{-3} $M_\odot$ for lobe S3 of He 2-47 and lobe N2 of M1-37 (all masses scale as $D^{2.5}$), respectively. The masses of the other major lobes are comparable. These lobes have probably been produced fairly recently—although we do not know their expansion histories, we estimate very rough expansion ages of ~180–500 yr by dividing their linear extents, (1.1–1.5) $\times$ 10^{17} cm, by a velocity of 100–200 km^{-1}, typical of the outflow velocities found for the fast bipolar outflows seen in PPNs such as CRL 2688, OH 231.8+4.2, and M1-92 (Alcolea et al. 2000).

In He 2-47, we find the density of the rings to be about 3.4×10^4 cm^{-3} from their excess (over the neighboring nebulosity) Hα brightness (~3.5×10^{-12} ergs s^{-1} cm^{-2} arcsec^{-2}), assuming their line-of-sight thickness to be equal to their average width (~4 pixels = 0″.18). In M1-37, the average waist density and mass are about 8.2×10^3 cm^{-3} and 1.6×10^{-4} $M_\odot$, respectively, if we model it as an edge-on torus with a thickness and diameter of 3 and 25.5 pixels, respectively.

3. THE PROGENITOR AGB STARS: NEUTRAL NEBULAR MASS AND MASS-LOSS RATES

The *IRAS* broadband photometric fluxes of both PNs signify the presence of substantial cool dusty CSEs around the central star; the faint round halos seen in our *HST* images directly show their presence. The halos are most likely due to scattering of Hα emission from the bright central regions by dust in the AGB CSEs. The color-corrected *IRAS* fluxes for He 2-47 are 15.7, 27.9, 46.5, and 3.8 Jy at 12, 25, 60, and 100 μm, respectively, and the *K*-band flux is 0.06 Jy (Acker et al. 1992). The Midcourse Space Experiment (MSX) point-source catalog (Egan et al. 1999) lists broadband fluxes of 1.2, 4.0, 5.9, and 39.3 Jy, respectively, in the *A* (8.3 μm), *C* (12.1 μm), *D* (14.6 μm), and *E* (21.3 μm) bands, consistent with the *IRAS* fluxes. We have estimated the dust mass by fitting these fluxes using a multicomponent dust emission model (Sahai et al. 1991). A dust emissivity of 150 cm^2 g^{-1} at 60 μm (Jura 1986), with a λ^{-p} power-law variation and $p = 1$ and 1.5 (characteristic of amorphous grains), has been assumed. We find that a good fit to all the fluxes requires at least two different temperature dust components. The dust mass (M_d) and temperature of the "cool" component are 2.0 (1.7) $\times$ 10^{-4} $M_\odot$ and 101 (112) K for $p = 1.5$ (1.0). For the "warm" component, only one constraining data point (namely, the *K*-band flux) is available in the short-wavelength region, and the poorly determined temperature and mass are $\gtrsim$500 K and $\lesssim 10^{-8}$ $M_\odot$, respectively. For M1-37, *IRAS* detected only 25 and 60 μm fluxes (8.47 and 9.2 Jy, respectively) and gave upper limits at 12 and 100 μm (<2.5 and <94.2 Jy, respectively); MSX measured *A*- and *E*-band fluxes of 0.14 and 5.8 Jy, respectively, with upper limits of 1.4 and 1 Jy in the *C* and *D* bands, respectively. We determine a rough dust mass and temperature of 5×10^{-4} $M_\odot$ and 90 K ($p = 1.5$) for M1-37. The luminosity estimated from the modeled infrared fluxes in these two objects is 840 and 1100 $L_\odot$, respectively, for He 2-47 and M1-37; the total luminosities are likely to be a factor of ~2.5 times larger, based on a model of the spectral energy distribution of M1-37 (Zhang & Kwok 1991).

Since the size of the far-infrared dust-emitting region θ_d is unknown, we assume that the warm dust is associated with neutral gas outside the ionized region (of size θ_i) and that $\theta_d \sim 2\theta_i$ (see, e.g., ST98). Thus, the dust ejection timescale $t_{\rm exp} = D(\theta_d - \theta_i)/(2V_{\rm exp}) = D\theta_i/(2V_{\rm exp})$, where $V_{\rm exp}$ is the CSE's expansion velocity. If we estimate θ_i as the geometric mean of the nebular extent along the waist and perpendicular to it, and if we take $V_{\rm exp} = 15$ km s^{-1}, typical of the neutral envelopes of PNs, we get $t_{\rm exp} \sim 2000$ yr for both nebulae. Thus, the progenitor AGB mass-loss rates in He 2-47 and M1-37, estimated as $dM_{\rm AGB}/dt = M_d\eta/t_{\rm exp}$ (where $\eta = 200$ is a typical gas-to-dust ratio for AGB CSEs), are ~2×10^{-5} and 5×10^{-5} $M_\odot$ yr^{-1},

respectively. Since the distances to our objects are relatively uncertain, we note that $M_d \propto D^2$ and $dM_{\rm AGB}/dt \propto D$.

4. DISCUSSION

In the popular model for the formation and shaping of PNs—the "generalized interacting stellar wind" (GISW) model—an aspherical PN results when a fast (1000–2000 km s^{-1}) spherical stellar wind from the post-AGB central star sweeps up material in a slowly expanding AGB CSE with an equatorial density enhancement (Balick 1987). Since the GISW model produces bipolar shapes with cylindrical symmetry around an axis orthogonal to the equatorial plane, it cannot explain the complex multipolar shapes and symmetries of the Starfish Twins (§ 2). Not only He 2-47 and M1-37 but *all* of the PNs imaged in our *HST* Hα survey have shown highly aspherical morphologies. The complexity, organization, and symmetries of these structures has led us to propose that the primary agents for shaping PNs are high-speed collimated outflows or jets that operate during the late AGB and/or early post-AGB evolutionary phase (ST98). These outflows carve out a complex *density imprint* within an intrinsically spherical AGB CSE. Subsequent expansion of a hot, higher velocity tenuous stellar wind from the post-AGB star inside the imprinted AGB CSE then produces the observed PN, whose shape and structure depend in detail on how the jet characteristics changed with time. The dense wall, tenuous interior structure of the lobes in the Starfish Twins is characteristic of that expected by the action of a collimated fast wind expanding inside a dense, slowly expanding CSE (thus, most of the mass in the lobes is due to swept-up gas).

Mechanisms for producing jetlike outflows, directly or indirectly, require the presence of a close binary companion. The most promising ones are those in which the outflows are (1) accretion disk–driven (e.g., Morris 1987; Soker 1996; Soker & Livio 1994) or (2) magnetohydrodynamically collimated by a stellar toroidal magnetic field (e.g., Garcia-Segura 1997; Różyczka & Franco 1996). The jet axis may change, in the first case, because of a radiation-induced instability that can warp the accretion disk, causing it to precess or wobble (Livio & Pringle 1997) and, in the second case, because of precession of the mass-losing star's rotation axis due to a binary companion. The Starfish Twins' multilobed structure suggests that the fast outflow changes its direction episodically and/or that multiple collimated outflows with different axes operate (quasi)simultaneously. The roughly equal radial extents of the major lobes in the Starfish Twins are indicative of the latter process, evidence for which is also found in three other PPNs, CRL 2688 (Cox et al. 2000), Roberts 22 (Sahai et al. 1999d), and the Frosty Leo Nebula (Sahai et al. 2000a).

The mechanisms for producing the dense waists or the offsets of the central stars from their centers are unclear. We have reported such offsets in the case of two other young PNs, the Etched Hourglass Nebula (Sahai et al. 1999b) and He 2-113 (Sahai, Nyman, & Wootten 2000b). Sahai et al. 1999b have discussed various physical mechanisms that could produce the offset in the Etched Hourglass Nebula and conclude that the most likely scenario would require a close binary companion; we speculate that the same may be true for the Starfish Twins. N. Soker, J. Kiger, & S. Rappaport (2000, in preparation) have discussed in detail the role of binarity in producing departures from axisymmetry and dislocation of the central stars from the nebular center. Although binarity has often been invoked to explain the presence of dense waists, it appears unlikely that the peculiarities of the waist structure in He 2-47 could be produced by mechanisms that *simply enhance the mass loss in the equatorial plane* through the presence of a close companion, such as gravitational focusing of the AGB wind (Morris 1987) or common envelope ejection (Livio 1993). Enhanced mass loss from cool magnetic spots in the star's equatorial zone can also produce a dense waist (Soker 1998) but seems unlikely for producing He 2-47's waist because it would require a rather contrived temporal-spatial configuration of the cool spots around the stellar equator. Hydrodynamic sculpting by the collimated outflows that produce the lobes may be required to further concentrate and shape the enhanced-density equatorial region in order to produce the observed waist structure.

In summary, *HST* imaging of the circumstellar environment in planetary and proto–planetary nebulae has brought renewed interest to the enterprise of understanding the physical phenomena that govern mass loss during AGB and post-AGB evolutionary phases and that shape its symmetry. Drastic modifications of existing theories or completely new ideas are needed in order to obtain a full understanding of the salient morphological features of PPNs and young PNs revealed by *HST*. The Starfish Twins are superb examples of the organized structural complexity that a new theory of PN shaping must address. Spectroscopic observations to probe the detailed kinematic structure of these compact PNs, possible only with the Space Telescope Imaging Spectrograph on *HST*, are urgently needed.

The author thanks Noam Soker and Adam Frank for critically reading this Letter and NASA for financial support of this work, provided through grant GO-0353.01-95A from the Space Telescope Science Institute (operated by AURA, Inc., under NASA contract NAS5-26555) and a Long Term Space Astrophysics grant (399-30-61-00-00).

REFERENCES

Acker, A., Ochsenbein, F., Stenholm, B., Tylenda, R., Marcout, J., & Schohn, S. 1992, Strasbourg-ESO Catalog of Galactic Planetary Nebulae (Garching: ESO)
Alcolea, J., Bujarrabal, V., Castro-Carrizo, A., Sanchez Contreras, C., Neri, R., & Zweigle, J. 2000, in ASP Conf. Ser. 199, Asymmetrical Planetary Nebulae II: From Origins to Microstructures, ed. J. H. Kastner, N. Soker, & S. A. Rappaport (San Francisco: ASP), 347
Balick, B. 1987, AJ, 94, 671
Bowers, P. F., Johnston, K. J., & Spencer, J. H. 1983, ApJ, 274, 733
Cox, P., et al. 2000, A&A, 353, L25
Egan, M. P., et al. 1999, Air Force Res. Lab. Tech. Rep. AFRL-VS-TR-1999-1522
Frank, A. 2000, in ASP Conf. Ser. 199, Asymmetrical Planetary Nebulae II: From Origins to Microstructures, ed. J. H. Kastner, N. Soker, & S. A. Rappaport (San Francisco: ASP), 225
Garcia-Segura, G. 1997, ApJ, 489, L189
Jura, M. 1986, ApJ, 303, 327
Livio, M. 1993, in IAU Symp. 155, Planetary Nebulae, ed. R. Weinberger & A. Acker (Dordrecht: Kluwer), 279
Livio, M., & Pringle, J. 1997, ApJ, 486, 835
Maciel, W. J. 1984, A&AS, 55, 253
Manchado, A., Stanghellini, L., & Guerrero, M. A. 1996, ApJ, 466, L95
Morris, M. 1987, PASP, 99, 1115
Różyczka, M., & Franco, J. 1996, ApJ, 469, L127
Sahai, R. 1999, ApJ, 524, L125
———. 2000, in ASP Conf. Ser. 199, Asymmetrical Planetary Nebulae II: From Origins to Microstructures, ed. J. H. Kastner, N. Soker, & S. A. Rappaport (San Francisco: ASP), 209
Sahai, R., & Bieging, J. H. 1993, AJ, 105, 595

Sahai, R., Bujarrabal, V., Castro-Carrizo, A., & Zijlstra, A. 2000a, A&A, in press
Sahai, R., Bujarrabal, V., & Zijlstra, A. 1999a, ApJ, 518, L115
Sahai, R., et al. 1999b, AJ, 118, 468
Sahai, R., Nyman, L.-A., & Wootten, A. 2000b, ApJ, in press
Sahai, R., te Lintel Hekkert, P., Morris, M., Zijlstra, A., & Likkel, L. 1999c, ApJ, 514, L115
Sahai, R., & Trauger, J. T. 1998, AJ, 116, 1357 (ST98)
Sahai, R., Wootten, A., Schwarz, H. E., & Clegg, R. E. S. 1991, A&A, 251, 560
Sahai, R., Zijlstra, A., Bujarrabal, V., & te Lintel Hekkert, P. 1999d, AJ, 117, 1408
Schwarz, H. E., Corradi, R. J. M., & Melnick, J. 1992, A&AS, 96, 23
Soker, N. 1996, ApJ, 468, 774
———. 1998, MNRAS, 299, 1242
Soker, N., & Livio, M. 1994, ApJ, 421, 219
Zhang, C. Y., & Kwok, S. 1991, A&A, 250, 179